81-GT-94

AN ASME PUBLICATION
$4.00 per copy $2.00 to ASME Members

THE AMERICAN SOCIETY OF MECHANICAL ENGINEERS
345 E 47 St., New York, N.Y. 10017

F. K. Tsou
Professor,
Department of Mechanical Engineering
and Mechanics,
Drexel University,
Philadelphia, Pa.
Mem. ASME

L. T. Smith
Assistant Professor,
Department of Mechanical Engineering,
University of Hartford,
West Hartford, Conn.
Mem. ASME

S. J. Chen
Graduate Student,
Department of Mechanical Engineering
and Mechanics,
Drexel University,
Philadelphia, Pa.

Experimental Determination of Transition Reynolds Number for Unsteady Film Cooling*

In order to investigate the unsteady effect on transition in film cooling, an 11-m long Ludwieg Tube, consisting of a test section placed between the high pressure and low pressure sections of a shock tube, has been constructed. With this device, a controlled unsteady, low subsonic flow lasting for a period of several milliseconds is obtained. The transition Reynolds Number is determined from the output of thin film heat flux transducers having a response time of a fraction of a microsecond. The results indicate that, in the case of flow without gas injection into the boundary layer, the transition Reynolds Number is one order of magnitude smaller than the critical Reynolds Number for steady wedge flow with the same pressure gradient. With injection, the transition Reynolds Number is small near the injection slot; far downstream, it increases asymptotically to the value for flow without injection.

NOMENCLATURE

a	speed of sound
	distance for the wave head (or leading edge) to a location in the downstream
M	Injection parameter = $\frac{}{p_s U_s}$
M	mass flow rate
P	pressure
P_a	atmospheric pressure
P1'132'•••136	position of the pressure transducer (see Figs. 3 and 4)
Re_c	critical Reynolds Number = P_n / P
Re_t	transition Reynolds Number = Pljk
s	slot height (see Fig. 11)
T	temperature
T $T_{2'}$ ...T_7	position of the thin film heat flux transducer (see Figs. 3 and 4)
t	time
t_w	defined in Fig. 5
x	horizontal coordinate (see Fig. 4)
x'	distance measured from the slot center line to a location in the downstream
U	free stream velocity
U_i	velocity of the injection stream
U_s	free stream velocity when the steady state has been reached in the test section
V	volume of the injection cylinder
a	injection angle (Fig. 3)
S	dimensionless pressure gradient - $\frac{po-p\ s}{P_{a\ 2'}}$
	ratio of specific heats
	similarity parameter = 1 $\frac{}{a\ t_o}$
	density
Ps	free stream density when the steady state has been reached in the test section

SUBSCRIPTS

i	injection stream
o	high pressure supply section
w	wave head

*Supported by National Science Foundation.

Contributed by the Gas Turbine Division of THE AMERICAN SOCIETY OF MECHANICAL ENGINEERS for presentation at the Gas Turbine Conference & Products Show, March 9-12, 1981, Houston, Texas. Manuscript received at ASME Headquarters December 11, 1980.

Copies will be available until December 1, 1981.

INTRODUCTION

The method of film cooling in steady boundary layers has been studied extensively in the past years. Film cooling investigations in an unsteady boundary layer, i.e., unsteady film cooling, have not been reported in the literature except for a few analyses [1, 2, 3]. It has been found that if the time involved in the process is in the order of one millisecond or shorter, the transient effect is considerable. To explain this point, we describe the following two unsteady film-cooling problems:

A. Gas Turbine Blade Cooling

In a gas turbine, the viscous wakes shed from a row of stationary (or rotor) blades will interact with the flow past a rotor (or stationary) blade of the next row. This interaction between blade rows results in periodic fluctuation of the free stream velocity and pressure distribution over each blade. Based on an unsteady air foil theory for two-dimensional incompressible flow through cascades, Meyer [4] obtained a free-stream velocity distribution that was sinusoidal in both time and streamwise coordinates. The calculated velocity amplitude is approximately 10% of the mean value. Owing to the fast blade motion, the frequency for a typical gas turbine application is in the order of ten KHz or higher, i.e., the time involved in such a motion is in the order of 0.1 ms or less. Based on a periodic free-stream velocity variation with a period of 2 ms, the unsteady film-cooling effectiveness was calculated [1]. The results indicate that the variation of the effectiveness is stronger than that of the input free-stream velocity variation. However, for large time period, say one second, the results show no discernable difference between the calculated unsteady film-cooling effectiveness and the steady film-cooling effectiveness based on average free-stream velocity, i.e., the unsteady effect is negligible for such a large time period.

B. Gun Barrel Cooling

The transient film-cooling process applied to gun barrels was described in an early work [2] and its effectiveness was predicted. In this application, a thin layer of ablative material is wrapped around the propelling charge. When the high temperature gas is produced during combustion, the material degrades to form a cool gas film that flows along the barrel and separates the high temperature core flow from the barrel surface. In this way, the effect of film cooling is obtained and the barrel erosion in the vicinity of the breech is significantly reduced. The time involved in such a process is again in the order of one millisecond. The calculated results of the unsteady film-cooling effectiveness indicate a considerable cooling effect even after the coolant injection has been stopped.

Thus, in the case of gas turbine blade cooling and gun barrel cooling, the unsteady effect is important. In his presentation on fundamental mechanisms that affect the estimate of heat transfer to gas turbine blades, Graham [5] also indicates that one of the most important influences on the local heat transfer distribution on the leading edge of the pressure and suction surfaces of a turbine vane or blade is the time-unsteady condition of the flow as it enters the blade or vane row. In order to have better understanding of such an effect, the experimental investigation of unsteady film-cooling was conducted. The results of one phase of the research, namely the determination of transition Reynolds number, are reported in this paper.

A brief description of our experimental equipment and objectives is in order. An intermittent wind tunnel referred as the Ludwieg Tube was designed, constructed, and installed. The Ludwieg Tube contains a test section placed between the high pressure section and the low pressure section of a shock tube such that a well-controlled flow will be achieved. This flow will last for a period of several millisecond or longer, i.e., a period comparable to that used in the analyses.

Instrumentation described in the later sections includes piezo-electric pressure transducers for pressure measurements and thin film transducers for wall heat-flux measurements. The latter transducer has a response time of less than one microsecond and is thus suitable for determining the nature of the boundary layer, i.e., whether it is laminar, transitional, or turbulent. For details of the technique, interested readers are referred to the work of Nagamatsu, et al [6].

It is of primary importance to understand the nature of the boundary layer prior to the studies of unsteady flows with injection. This paper, the first of a series on unsteady film-cooling, is thus concerned with an experimental determination of transition Reynolds Number with and without film-cooling. Such transition Reynold Numbers were obtained from oscilloscope recordings of pressure transducer and heat flux transducer output.

DESCRIPTION OF EXPERIMENTAL FACILITY AND INSTRUMENTATION

The experiments were carried out in the Ludwieg tube intermittent wind tunnel shown in Fig. 1. The tunnel consists of three sections: a 127 mm I.D. x 3 m pressure tube, a 127 mm x 100 mm rectangular cross section nozzle section fitted with viewing windows, and a 76 mm I.D. x 7 m dump tube. Transition sections, from circular to rectangular geometry, are used to provide smooth connections between the sections. Two-dimensional nozzles, having various geometries, are mounted in the nozzle section; a thin Mylar diaphragm separates the nozzle section and dump tube.

The operating stages of the configuration are shown in Fig. 2, an x-t diagram and sketch of the tunnel. When the diaphragm is broken at time zero, a shock wave followed by a contact surface travels downstream into low pressure gas in the dump tube. At the same time, an expansion wave propagates upstream into the pressure tube and accelerates the gas toward the nozzle. During this initial starting process, we have unsteady flow in the test section of the nozzle, with $U = U(x,t)$, for a period of several milliseconds. As soon as the nozzle throat becomes choked, the remaining part of the expansion wave is swept downstream and the expansion flow of gas through the nozzle becomes steady. The steady flow time in the nozzle is of the order of 10 to 15 milliseconds.

Details of the subsonic nozzles and gas injection system used in this investigation are shown in Fig. 3.

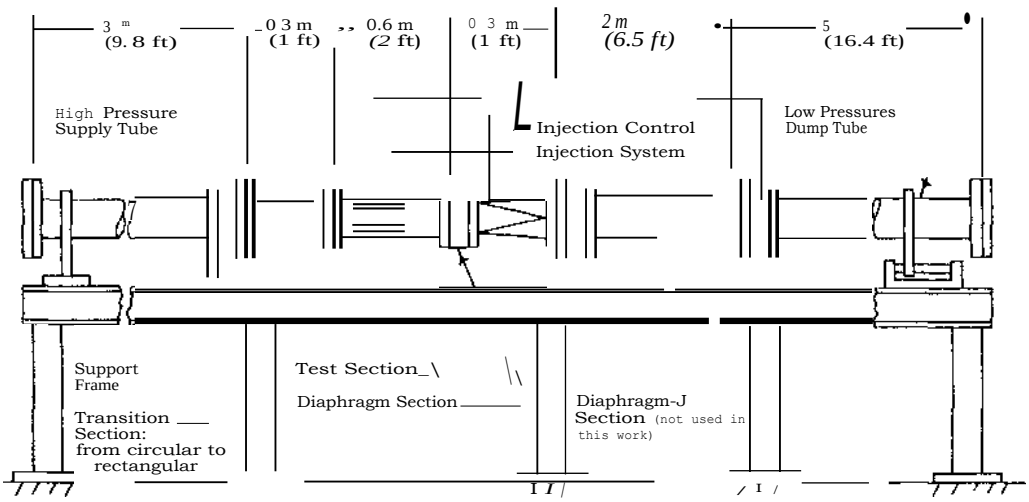

Fig. 1. Schematic drawing of Ludweig Tube facility.

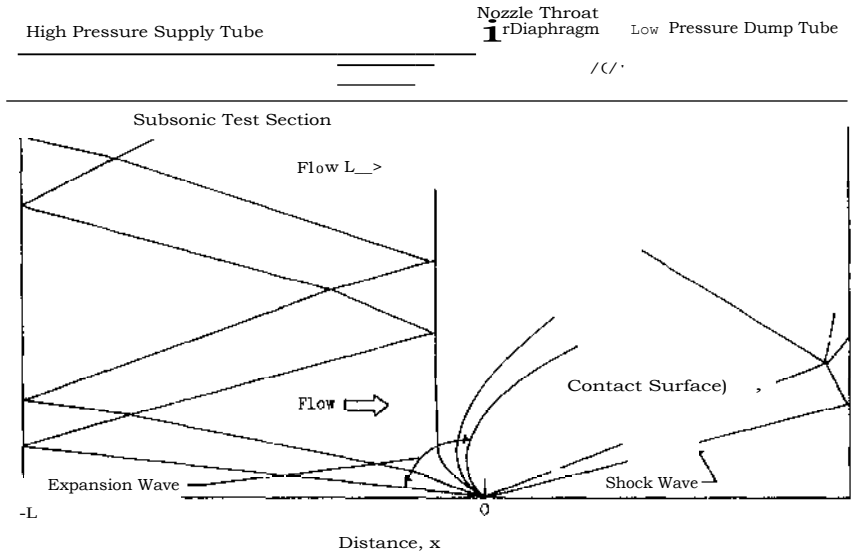

Fig. 2. The Ludwieg Tube intermittent wind tunnel: sketch and simplified x-t diagram.

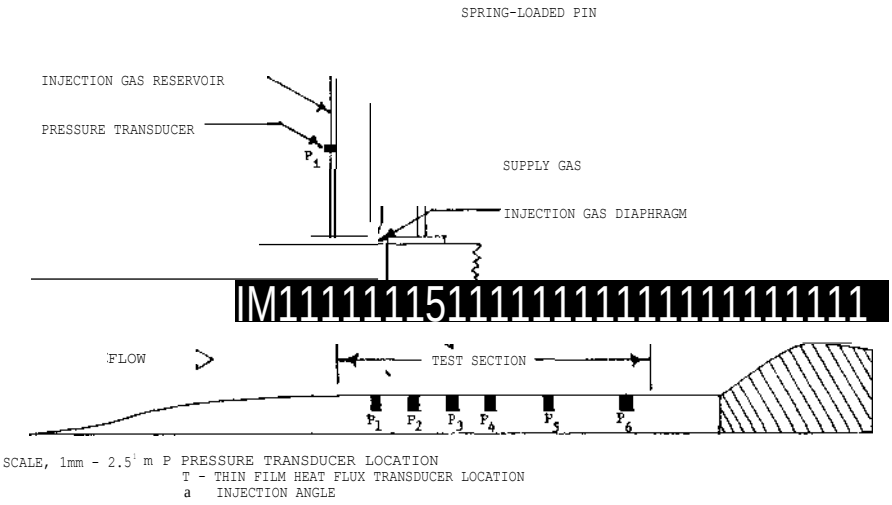

SCALE, 1mm - 2.5 m P PRESSURE TRANSDUCER LOCATION
T - THIN FILM HEAT FLUX TRANSDUCER LOCATION
a INJECTION ANGLE

Fig. 3. Nozzle blocks, subsonic test section, instrumentation, and gas injection mechanism.

The nozzle blocks were machined from solid aluminum blocks. The inlet contraction section of the nozzle was designed using the method developed by Tsien [7] to produce uniform velocity at the beginning of the straight wall test section. The test section is 50.8 mm in height and 127 mm wide to insure negligible side wall effects on pressure and temperature measurements conducted along the centerline of the nozzle blocks. The test section is followed by a converging diverging section, shown shaded in Fig. 3. With this section in place, a steady flow Mach number of 0.14 is produced in the test section. In order to vary the flow conditions in the test section, the converging-diverging portion of the nozzle is replaced by a straight wall section which preserves the area of the test section. In this configuration, the eventual steady flow Mach number is 0.4.

Also shown in Fig. 3 are the details of the gas injection slot and injection gas reservoir. The 3 mm x 38.1 mm injection slot is constructed of stainless steel and is mounted flush with the surface of the test section. Injection angles of 15 and 30 with respect to the horizontal direction are provided. The gas flows from the reservoir to the injection slot through a curved channel designed to prevent internal flow separation. The injection mass flow rate is determined by measuring the time rate of change of the injection gas reservoir pressure, dp./dt, during the run. For the short injection times involved (ti 10 to 15 milliseconds), the process within the injection gas reservoir can be assumed to be adiabatic [8]. The injection gas mass flow rate is then given by

$$m_i \quad \frac{V}{yRT} \frac{dpi}{dt} \qquad (1)$$

where, for small reservoir pressure drops, the injection gas temperature, T_i, may be considered constant [8]. Two methods of producing gas injection may be used. For one, the reservoir is left open to the test section prior to the start of the main flow. As the expansion wave passes over the injection slot, the decreasing main flow pressure causes injection gas to flow from the reservoir through the slot. The second method provides for higher injection mass flow rate. Here, the reservoir is sealed off by a Mylar diaphragm with reservoir pressure higher than the initial test section pressure. Injection gas flow is started by breaking the diaphragm with a spring - loaded pin, and the injection flow may be initiated prior to the start of the main flow or at various times during the transient main flow.

Measurements of pressure as a function of time in the test section and the injection gas reservoir are made using Kistler Model 60381 quartz piezoelectric pressure transducers. These are mounted flush with the lower test section wall, at locations shown in Fig. 3, in mounts designed to minimize mechanical shock. The response time of the transducers is of the order of 1 microsecond.

Wall temperature and heat flux are measured as a function of time at several locations in the test section (see Fig. 3) using their film heat flux transducers made of platinum bonded to a Pyrex substrate. The transducers, manufactured by Medtherm Corporation, have a response time of less than 1 microsecond and are thus suitable for heat flux and boundary layer transition measurements during the millisecond unsteady flows considered in this investigation. The thickness of the platium film is 1000 and the films are mounted flush to the test section wall, along the centerline, with their long axis perpendicular to the direction of flow. Oscilloscope recordings of both pressure transducer and heat flux transducer output are photographed for subsequent analysis.

Unless otherwise stated, the x-coordinate used in this work is measured from the origin of the coordinate system toward the test section. The free-stream velocity, U is therefore in the negative x-direction (see Fig. 4). The distances from the injection slot and each transducer to the diaphragm are also given in the figure. The location of the origin of the coordinate system will be described in later sections.

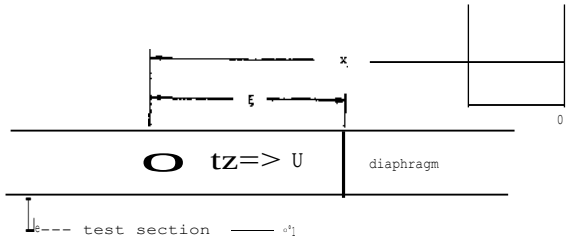

Location of the transducers:

Transducers	ξ(cm)	Transducers or slot	x (mm)
T_1	450.85	P1	400.05
1_7	370.15	P2	374.65
T_3	362.66	P3	349.25
T_4	350.65	P4	323.83
T_5	329.'64	P5	285.75
T_6	274.24	P6	234.95
T_7	239.65	slot	374.65

Fig. 4. Coordinate System and the locations of all transducers (see Fig. 3 for T's and P's).

EXPERIMENTAL RESULTS

To conduct the experiment, we first evacuate the whole system (see Fig. 1) to a low pressure corresponding to the initial pressure in the dump tube. The high pressure supply tube is then filled with dry air to pressure p_o. When the diaphragm is raptured, an unsteady flow lasting several milliseconds is produced in the test section. To produce injection dry air flow, the initial reservoir pressure is set equal to the initial pressure p in supply tube. The reservoir is then sealed off ?rom the injection gas supply cylinder. The injection diaphragm indicated in Fig. 3 is therefore not used and gas injection is generated by the decreasing main flow pressure during the run. Three different supply pressures, p = 68.95 KPa(10.0 psia), 101.3 KPa(14.7 psia) and ?34.5 KPa (19.5 psia), were used in the experiments.

A Tektronix quadri trace oscilloscope is used to obtain photographic recordings of pressure transducer and thin film heat flux transducer output. Often two

pressure traces and two heat flux traces can be arranged clearly in one photograph (see Fig. 6b). The pressure traces are used to obtain the information on the free-stream pressure and velocity and the injection stream mass flow rate while the heat flux trace is employed to determine the time and location where boundary layer transition takes place. Quantitative information on wall heat transfer rates and wall temperature is not needed in the present work.

To understand some details of the oscilloscope output, we refer to the sketch given in Fig. 5,

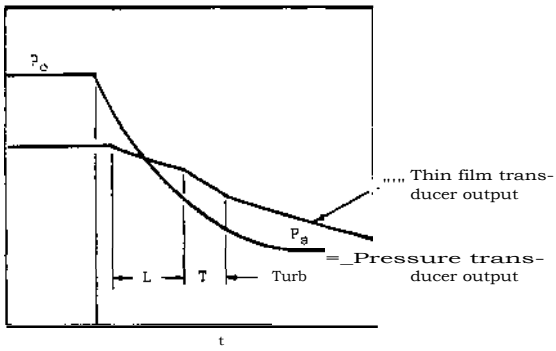

Fig. 5. Sketch for typical oscilloscope trances of a pressure transducer output and a thin film transducer output. L = laminar boundary layer, T = transition zone; Turb = turbulent boundary layer.

where both pressure and heat flux gage output are shown. When the diaphragm is raptured, the expansion waves propagate toward the nozzle test section. At time t_w shown in the figure, the wave head reaches the loc ation of the pressure transducer under consideration. The pressure p and the sound speed a are the initial conditions in the high pressure supply tube. For time greater than t_w the pressure vs. time output of the transducer serves to measure the time development of the unsteady main flow at the location of the transducer. The pressure drops from p to a steady state value p_s in a period of several milliseconds. The time derivative 303t from the pressure transducer output is constant near the early stage of the pressure drop. The results of measurements also indicate that the pressure gradient, 8p/8x is also a constant in the neighborhood of the wave head.

The output of the thin film heat flux transducer as sketched in Fig. 5 has another significant meaning. Because of its fast response (in a fraction of one microsecond), this transducer is able to respond according to the nature of the boundary layer, i.e., laminar, transitional, or turbulent. As shown in Fig. 5, the time at which transition takes place can then be determined by the abrupt change in the slope of transducer output vs. time curve.

A. Free-Stream Pressure and Velocity

With these sketches in mind, one may examine two typical photographic oscilloscope recordings given in Figs. 6a and 6b. The top and middle cures of Fig. 6a represent output from the pressure transducers, P_3 and P_4 respectively, the supply pressure p_o for each curve being 101.7 KPa (14.75 psia). The pressure drop from p to the steady-state pressure p takes place in a period of slightly more than 2 ms. he time derivative, 909t is approximately constant except in the beginning and near the end of the pressure drop. The bottom curve of Fig. 6a represents output of the heat flux transducer T_5. The transition time as seen from the figure is about 1.3 ms later than the time when the wave head arrives at the location of the transducer T_5. There was no injection flow in this case.

Fig. 6b shows the unsteady boundary-layer flow with injection through the slot. The top curve shows the drop of the injection cylinder pressure, p_i, which is seen to be linear with t. The injection mass flow rate M calculated from Eq. (1) is therefore a constant. The second curve represents output from the pressure transducer p_4. The third and the bottom curves show the output from heat flux transducers T_4 and T_7 The transition times are again clearly indicated.

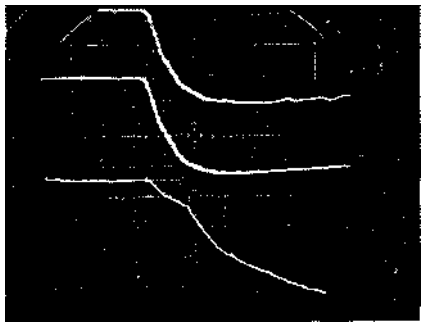

Fig. 6a. Top two curves - output from P_3 and P_4, 13.79KPa(2 psi)/div.t
Bottom curve - output from T_5, 0.2mv/div.t
Time scale - lms/div.±

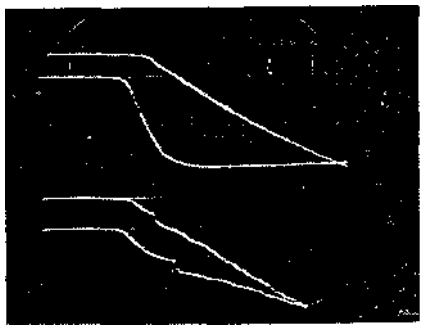

Fig. 6b. Top curve - output from Pi, 6.89KPa(lpsi)/ div.t
2nd curve - output from P_4, 13.79KPa(2psi)/ div.t
3rd and bottom curves - output from T_4 and T_7, 0.2mv/div.4
Time scale - lms/div.±

The data reduction methods used to obtain free stream pressure and velocity as functions of the similarity parameter n are as follows: Let the origin of the x-t coordinate system be the time and location at which the expansion wave starts to propagate (Fig.4).

At time t , the expansion wave head reaches to the location of a transducer. One may calculate t_w from the relation,

$$t_w = x_w / a_o \quad (2)$$

where x_w is the distance from the origin to the transducer. The location of the origin is not arbitrary but is uniquely determined from the equation,

$$x_w = -\frac{1}{\gamma+1} p_o a_o / (\quad) \quad (3)$$

where the value of the first derivative of pressure at the wave head, $(Dp/@t)_w$ is measured from the pressure traces. The origin determined in this way is located to the right of the diaphragm (Fig. 4), the distance between the origin and the diaphragm being approximately lm for high pressure runs and 0.75m for lower pressure runs. Eq. (3) is derived from simple wave equations and isentropic relations [11].

The dimensionless pressure p/p obtained from the pressure traces is then plotted versus n(= 1 - x/a_ot) in Fig. 7, where data points for flow

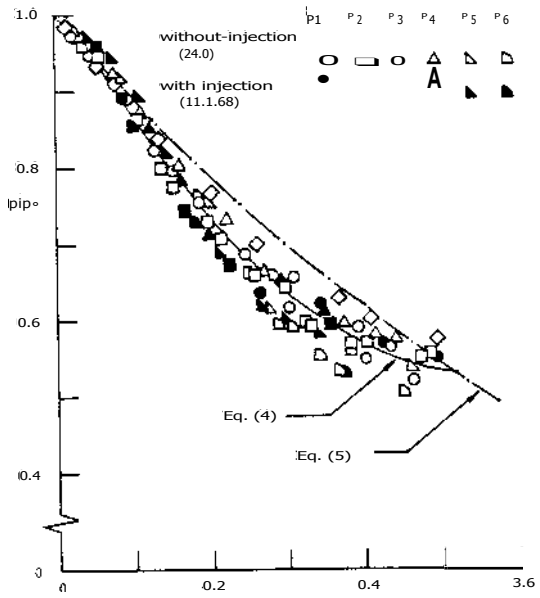

Fig. 7. Dimensionless pressure p/p_o versus n for p_o = 101.3 KPa.

without injection, M=0 and with injection, M=1.68 (average value) for all pressure transducers output are shown. The supply pressure p used in these runs was 101.3KPa (14.7 psia). For the purpose of data fitting, the following second degree polynominal resulting from least square approximation is indicated in the figure,

$$\frac{P}{P_o} = 1.026 - 1.776\ n + 1.579\ n^2 \quad (4)$$

To compare this experimental curve with the theory, the center expansion wave solution,

$$P_o = (1 - \frac{\gamma-1}{\gamma+1} n)^{\frac{2\gamma}{\gamma-1}} \quad (5)$$

is also plotted in Fig. 7, where the specific heat ratio y was taken as 1.4.

The data points of p/p_o are utilized to calculate the dimensionless free stream velocity, U/a_o. The results of the calculation based on the solution of one-dimensional characteristic equations,

$$\frac{U}{a_o} = \frac{2}{\gamma-1}\left(1 - \frac{a}{a_o}\right) \quad (6)$$

and isentropic relations are presented in Fig. 8.

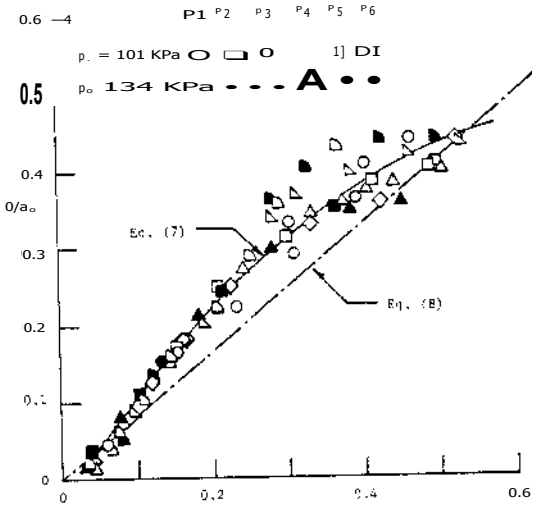

Fig. 8. Dimensionless Free stream velocity U/a_o versus n for cases without injection.

The least square fit indicated in the figure has the form,

$$\frac{U}{a_o} = 0.026 + 1.441\ n - 1.043\ n^2 \quad (7)$$

The center expansion wave solution,

$$\frac{u}{a_o} = \frac{2}{\gamma+1} n \quad (8)$$

is again plotted in the figure for comparison.

Further discription of Figs. 7 and 8 are made: (1) In both figures, data scattering occurs in the range, 0.3 < n < 0.5, i.e., the flow may not be quite similar in this range. (2) Comparison of the curves with the theoretical curves of center expansion wave appears reasonable. The maximum deviation is less than 10%. The trend of both curves, however, is seen to be different. Such a difference is due to the

effect of non-center expansion waves in the present experimental facility. A description of the non-center waves is given elsewhere [11]. (3) For the sake of space saving, the data of pressure with and without injection at one supply pressure p is presented in Fig. 7 while the results of free stream velocity without injection but with two different supply pressures are given in Fig. 8. (4) There is no discernable effect of injection flow on the free-stream pressure as observed from Fig. 7. This situation is consistent with the concept that the mixing of both streams takes place inside the boundary layer without having influence on the free stream properties [12]. (5) Data presented in both figures was obtained by using a straight wall section to replace the converging-diverging section shown shaded in Fig. 3.

B. Transition Reynolds Number

To obtain experimental transition Reynolds Number, we first measure the transition time from the output of the thin film transducer. The similarity parameter, p is next calculated. The dimensionless pressure, p/p_o and velocity, U/a are calculated, respectively, from Eqs. (4) and b). The transition Reynolds Number, Re = pUk/p, can then be computed. The characteristic iength, **I**, in the definition of Re_t is the distance from the wave head to the location of the thin film transducer at the transition time.

In the absence of injection, Re_t is plotted versus the average dimensionless pres sure gradient 8 in Fig. 9.

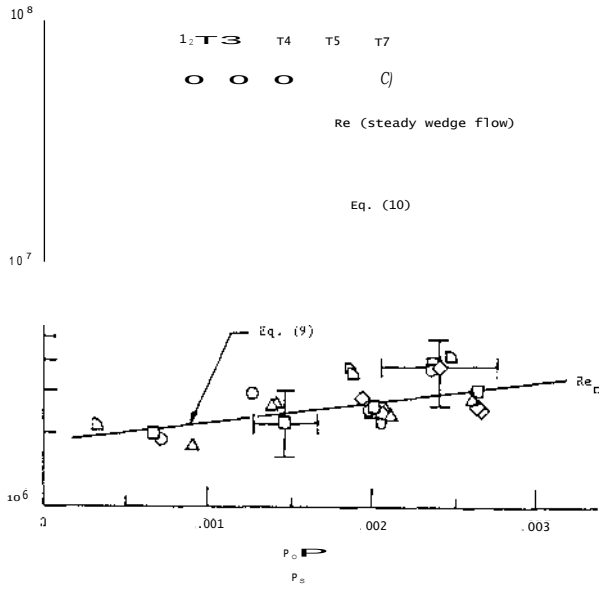

Fig. 9. Transition Reynolds Number, Re and critical Reynolds Number, Re versus the dimensionless pressure giadient (without injection)

A least squares fit of the data yields the empirical relation,

$$Re_t = (1.84 \times 10^6) \exp[189\ 8] \quad (9)$$

In each experiment considered, the pressure gradient, ap/Dx, is favorable; it is also constant in the region close to the wave head. Fig. 9 indicates that Re_t increases as (3 increases. Such a trend is similar to the case of a steady boundary layer.

In view of the apparent lack of analytic or experimental investigations dealing with transition in the type of unsteady flow considered here, we have chosen to compare the present measured Re in unsteady boundary layers with the Reynolds Numher at the point of instability (or critical Reynolds Number Re_c) in steady wedge flows with constant pressure gradients. The solution of Re_c [9] based on the Orr-Sommerfeld equation is shown as the top curve in Fig. 9. To construct this solution curve, we take the following precedures: (1) utilize the measured pressure gradient 8 for the wedge flow shape factor calculation and (2) utilize properties for the wedge flow evaluated from the unsteady flow conditions at the transition time of the experiments. Re values are then obtained from the solution in Reg. 9. Because of the different property values, the calculated points did not fall precisely on a smooth curve. The curve presented in the plot was smoothed out by means of a least square fit. The final form of the equation is,

$$Re_c = 2.33 \times 10^7 \exp[120\ 8] \quad (10)$$

In comparing both curves in Fig. 9, one sees that the measured Re is one order of magnitude smaller than the calculated Re of steady wedge flow. The Re_t curve, however, hSs a slightly larger slope.

It has to be noted that Re depends on the local boundary layer thickness **6.** A hiscussion on the nature of **6** is therefore necessary. Owing to the limitation of the present experimental equipment, no boundary layer measurements can be conducted, that is, the measured **6** is not available. Consideration is then given to a power series solution [13] of the laminar boundary layer flow produced by the center expansion waves described in the foregoing. The boundary layer thickness **6** obtained from this solution will be used as an estimated **6** for the present measured flow. Such an estimation is expected to be reasonable since the measured free stream velocity and the theoretical free stream velocity of the center expansion wave flow are fairly close (see Fig. 8).

Calculation of **6** at several transition times have been performed from the solution. The results indicate that **6** for the present measured flow is smaller than that for the steady wedge flow by the amount of 21% to 36%. From these results, the critical Reynolds Number based on **6** of the steady wedge flow is again one order of magnitude larger than the transition Reynolds Number based on **6** estimated from the present measured flow. The comparison was made for the same pressure gradinet 8. The measured flow is therefore less stable.

In the presence of injection flow, i.e., with film cooling, two slot geometries, a = 15° and 30°, have been investigated. The injection parameter, M = p.U./p U, was kept approximately 1.68 for all runs. Wilh M being held constant, one finds that the measured Re is a function of the dimensionless pressure gradient 8, the injection angle a and the location of the transducer from the slot x'. The results are presented in Fig. 10, where Re_t is also seen to increase as S increases.

For a given location of the transducer, one observes that Re for **a = 15°** is higher than that for a = 30°. Their hifference, however, becomes small and finally diminishes in the far downstream where the

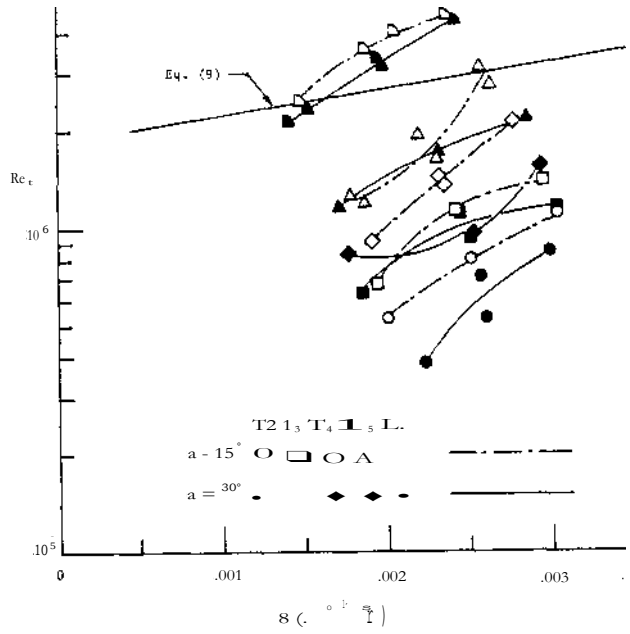

Fig. 10. Transition Reynolds Number, Re_t versus dimensionless pressure gradien$t$, δ_o for two injection angles (a = 15°, 30°) at various locations.

values of Re with and without injection are essentially the same. The latter situation is because the effect of injection becomes negligible in the far downstream. In the upstream locations, Re_t is smaller with injection. The effect of injection there is to produce S-shape boundary-layer velocity profiles and the resulting flow is therefore less stable.

Data reduction is made to bring together all experimental curves shown in Fig. 10. The resulting equation plotted in Fig. 11 has the form

$$Re_t = 89300 \left(\frac{x'}{s} \cos a\right)^{0.407} \exp[.485 \quad (11)$$

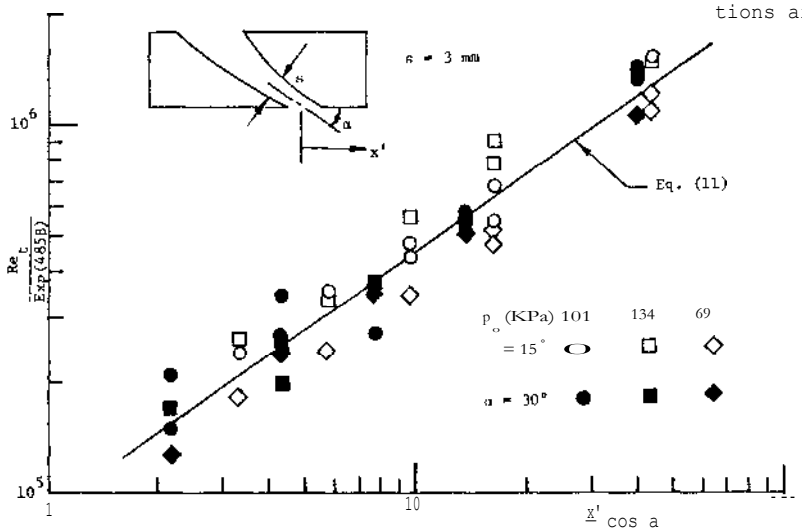

Fig. 11. Transition Reynolds Number Versus Dimensionless Parameter, x'/s cos a.

where x' is the distance measured from the slot centerline to a downstream location.

DISCUSSION AND CONCLUSION

It is important to determine the point of transition at which the boundary layer changes from a laminar to a turbulent state. This change will give rise to a significant effect on the aerodynamics performance of the solid surfaces as well as the local heat transfer rates. In the foregoing, the measurements of transition Reynolds Number in unsteady boundary-layer flow prevailing in the Ludwieg Tube with and without injection have been described. The low subsonic main flow with Mach Number up to 0.4 and, in the case of air injection through the slot, a strong injection with M = 1.68 have been utilized to obtain test data. The main flow lasts in a period of 2 to 3 milliseconds. The measurements have been made possible since the response time of the pressure and thin film heat flux transducers is in the order of one microsecond. The measured pressure gradient is constant at a given time and in all cases, the pressure gradient is favorable. The measured transition Reynolds Number results presented in the aforementioned figures, lead to the following final discussion and conclusion:

(1) The objective of this work is to investigate the unsteady effect on transition Reynolds Number. The parameters considered herein include the pressure gradient, injection angle, injection parameter and the distance from the slot. It is not intended to discuss other possible parameters in unsteady film cooling. A discussion of parameters, applied to the steady gas-turbine blade cooling for example, can be found elsewhere [5, 10].

(2) In the absence of injection, the measured value of Re_t one order of magnitude smaller than the critical Reynolds Number obtained from the steady wedge flow with same pressure gradient. The unsteady boundary layer under consideration is therefore less stable.

(3) In the sufficiently far downstream (x'/s ti 40), the results of Re_t with or without injection are very close, thus, th effect of far upstream injection is negligible. Re_t in other locations are smaller with injection.

(4) The effect of the injection angle on the measured Re_1 occurs essentially at the location near the slot where Re is larger for the smaller injection angle. This effeCt becomes small and finally diminished in the far downstream.

(5) The error bars shown in Fig. 9 represent computed estimated errors based on the accuracy to which we can read our instrumentation and oscilloscope recordings. The errors can be reduced significantly if the data acquisition system including a digital output equipment with a real time computer is used to replace the present method of employing the oscilloscope recordings.

REFERENCES

1 Tsou, F. K., T. Varghese, and L. C. Szema, "The Effect of Periodic Free-Stream Variation on Film Cooling" Proceedings 14th Annual Meeting of the Society of Engineering Science, Recent Advances in Engineering Science, ed. G. C. Sih, 1977, pp. 485-494.

2 Tsou, F. K., "Prediction of Film-Cooling Effectiveness in an Unsteady Turbulent Boundary Layer," ASME Paper, 76-HT-28.

3 Tsou, F. K. and T. Varghese, "Film Cooling with Injection from a Moving Projectile," Proceedings of the Second International Symposium on Ballistics," Daytona Beach, Florida, 1976.

4 Meyer, R. S., "The Effect of Wakes on the Transient Pressure and Velocity Distributions in Turbomachines," Transaction of the ASME, V. 80, 1958, p. 1544.

5. Graham, R. W., "Fundamental Mechanisms that influence the Estimate of Heat Transfer to Gas Turbine Blades," ASME paper, 79-HT-43.

6. Nagamatsu, H. T., B. C. Graber, and R. E. Sheer, "Roughness, Bluntness, and Angle-of-Attack Effects on Hypersonic Boundary-Layer Transition," J. Fluid Mech. V. 24, part 1, 1966 pp. 1-31.

7. Tsien, H. S., "On the Design of a Contraction Section for a Wind Tunnel," J. Aero, Sci., V. 10, 1943, pp. 68-70.

8. Jones, T. V. and D. L. Schultz, "Film Cooling Studies in Subsonic and Supersonic Flows Using a Shock Tunnel," 8th International Shock Tube Symposium, Imperial College of Science and Technology, London, England, 1971, pp. 13/1 - 13/12.

9. Schlichting, H., "Boundary Layer Theory" 7th ed. McGraw-Hill, 1980.

10. Seyb, N. J., "The Roll of Boundary Layers in Axial Flow Turbomachines and the Prediction of Their Effects," AGARD-AG-164, Boundary Layer Effects in Turbomachines, ed. J. Surugue, Paper 1-14.

11. Srinivasan, G., "Investigation of Laminar Wall Boundary Layers Developed Within Non-Centered Unsteady Waves," PhD dissertation, SUNY at Buffalo, 1974.

12. Spalding, D. B., "Prediction of Adiabatic Wall Temperatures in Film-Cooling Systems," AIAA J, V. 3, N. 5, May, 1965.

13. Cohen, N. B., "A Power Series Solution for the Unsteady Laminary Boundary Layer in an Expansion of Finite Width Moving Through a Gas Initially at Rest," NACA TN 3943, 1957.